

EFFECT OF Ni_3Ti FORMATION ON THE OXIDATION KINETICS OF NiTi SHAPE MEMORY ALLOYS

by

Nazihah Binti Nawawi

**Thesis submitted in fulfillment of the requirements
for the degree of
Master of Science**

OCTOBER 2014

**EFFECT OF Ni_3Ti FORMATION ON THE OXIDATION KINETICS
OF NiTi SHAPE MEMORY ALLOYS**

NAZIHAH BINTI NAWAWI

UNIVERSITI SAINS MALAYSIA

2014

ACKNOWLEDGMENTS

Foremost, I would like to express my sincere gratitude to my supervisor Dr. Abdus Samad bin Mahmud for his continuous support in my MSc study and research, for his patience, motivation, enthusiasm, and immense knowledge. His guidance helped me in all the time of research and writing of this thesis. Additionally, I would like to thank the rest principle investigators of the Nanofabrication and Functional Material research group: Dr. Khairudin bin Mohamed, Dr. Jamaluddin bin Abdullah and Dr Ramdziah binti Md Nasir for their encouragement.

My sincere thanks also goes to En. Zalmi, En. Shamsudin and En Latif for offering me the summer internship opportunities in their groups and leading me working on diverse exciting projects. I also thank my lab mates in the research group and all the postgraduate friends in USM for all the moral support and fun times we had together.

Last but not the least, I would like to thank my family: my parents Nawawi bin Abd Rahman and Yong Khasimah Sabarudin, for giving birth to me at the first place and supporting me spiritually throughout my life. Grateful thank to my beloved husband, Dr. Muhammad Haziq Zolkapli for the continuous support and love. Lastly, to my parents in-law, dear brothers and sisters who have taken care of my children Bilal and ‘Aqeel during the challenging writing phase in completing this study.

TABLE OF CONTENTS

Acknowledgments.....	ii
Table of Contents.....	iii
List of Tables.....	v
List of Figures.....	vi
List of Abbreviations.....	viii
List of Symbols.....	ix
Abstrak.....	x
Abstract.....	xiii

CHAPTER 1 – INTRODUCTION

1.1 Background.....	1
1.2 Problem statement and research interest.....	4
1.3 Objectives.....	6
1.4 Scope of work	7

CHAPTER 2 – LITERATURE REVIEW

2.1 NiTi shape memory alloy applications.....	8
2.2 Biocompatibility stability of NiTi in orthodontic arch wire.....	10
2.3 Sensitive composition dependent of NiTi phase transformation temperature.....	13
2.4 The effect of addition of other elements towards shape memory behaviour.....	15
2.5 Surface oxidation of NiTi shape memory alloy at elevated temperature.....	16
2.6 Sequential layer formation.....	20

2.7	Diffusion mechanism in oxide.....	24
2.8	Processing of shape memory alloy.....	25

CHAPTER 3 – RESEARCH METHODOLOGY AND EXPERIMENTAL WORK

3.1	Introduction.....	29
3.2	Materials.....	31
3.3	Sample preparation.....	31
3.4	Oxidation process.....	32
3.5	Thermal martensite phase transformation measurement.....	33
3.6	Surface morphology analysis.....	34
3.7	Thermogravimetric analysis.....	35

CHAPTER 4 – RESULTS AND DISCUSSION

4.1	Initial sample condition.....	37
4.2	The effect of time and temperature toward Ni_3Ti growth.....	40
4.3	Measurement of oxide weight gained.....	51
4.4	Martensite phase transformation behavior.....	53
4.5	Titanium oxidation rate profile.....	60
4.6	The origin of Ni_3Ti in NiTi system.....	64
4.7	The Ni_3Ti as a barrier to slower Ti diffusion.....	68

CHAPTER 5 – CONCLUSIONS

5.1	Conclusions.....	70
5.2	Recommendation for future works.....	72

References.....	74
-----------------	----

LIST OF TABLES

Table 2.1	Effect of Ni composition towards transformation temperature	14
Table 2.2	Amount of martensite and austenite for eight different arch wires	15
Table 3.1	List of specimen treated in air at various times and temperatures	33
Table 4.1	Table of Ni_3Ti thickness measured after oxidation	47
Table 4.2	Measurement for oxide thickness after treated at 800 and 900°C	62

LIST OF FIGURES

Figure 1.1	Schematic illustration of martensite phase transformations	2
Figure 2.1	SEM image of a NiTi wire treated in an oxidizing environment reveals three distinctive layers with TiO ₂ as the outermost layer	12
Figure 2.2	Three forms of TiO ₂ crystalline structure	16
Figure 2.3	a) EFTEM image of NiTi wire oxidized in air. White arrowheads are the thinner TiO ₂ capping b) HAADF image showing Ni particles in the TiO ₂ layer. Also seen are holes and cracks as indicated by the yellow arrows	18
Figure 2.4	Ni release from four types of surface treatments as a function of exposure time	19
Figure 2.5	Auger analysis of NiTi wire oxidized at 700 °C in air for an hour shows Ni concentration decreases with increasing depth from the surface	21
Figure 2.6	SEM images of the oxidation layers from a sample heat treated in 1 atm oxygen at 750°C for 4 hours	22
Figure 2.7	Schematic illustration of the layers formation during oxidation	23
Figure 2.8	Schematic procedure in NiTi shape memory alloys manufacturing	26
Figure 2.9	SEM images (BSE mode) of annealed orthodontic NiTi samples showing cracks parallel to the loading direction and disappears after unloading	28
Figure 3.1	The experimental flow	30
Figure 3.2	Thermal oxidation configuration scheme inside the furnace	32
Figure 4.1	SEM image of as-received NiTi wire cross sectional area	38
Figure 4.2	a) The elemental profile line plot of as-received NiTi wire cross sectional area	39

	b) The spot analysis of titanium oxide formed of the as-received wire	39
Figure 4.3	Thermal transformation behaviour of Ti-50.5at%Ni	40
Figure 4.4	Treatment at 700°C in air for different times	41
Figure 4.5	Treatment at 800°C in air for different times	43
Figure 4.6	Treatment at 900°C in air for different times	44
Figure 4.7	a) Ruptured oxide of specimen treated at 900°C for 60 minutes in air	46
	b) Measured oxide thickness of the specimen	46
Figure 4.8	Thickness growth for Ni ₃ Ti as treated at 700 – 900°C in air	48
Figure 4.9	EDS-SEM spot analysis result for TiO ₂ of specimen treated at 800°C	49
Figure 4.10	EDS-SEM spot analysis result for Ni ₃ Ti of specimen treated at 700°C	50
Figure 4.11	EDS-SEM spot analysis result for Ni ₃ Ti of specimen treated at 800°C	50
Figure 4.12	EDS-SEM spot analysis result for Ni ₃ Ti of specimen treated at 900°C	50
Figure 4.13	EDS-SEM spot analysis result for Ni(Ti) of specimen treated at 900°C	51
Figure 4.14	Plots for weight gained after treated at 700 - 900°C	52
Figure 4.15	Thermal transformation temperature of NiTi treated at 900°C in air	53
Figure 4.16	Effect of heat treatment temperature on transformation temperatures for samples heat treated in air at 900°C	54
Figure 4.17	Thermal transformation temperature of NiTi treated at 800°C in air	55

Figure 4.18	Effect of heat treatment temperature on transformation temperatures for samples heat treated in air at 800°C	56
Figure 4.19	Thermal transformation temperature of NiTi treated at 700°C in air	57
Figure 4.20	Effect of heat treatment temperature on transformation temperatures for samples heat treated in air at 700°C	57
Figure 4.21	Effect of oxidation towards transformation enthalpy change	59
Figure 4.22	Effect of oxidation towards A_s and M_s temperatures at all temperatures treated	59
Figure 4.23	Parabolic interpolation of TiO_2 formation during NiTi oxidation at 800 and 900°C in air	61
Figure 4.24	Formation of oxygen deficit TiO_2 , with oxygen ion vacancies and excess electrons from a perfect TiO_2	63
Figure 4.25	Schematic presentation of three main stages involved in NiTi oxidation	64
Figure 4.26	Schematics illustration of Ni_3Ti formation during the oxidation process	66
Figure 4.27	Growing behaviour of Ni_3Ti at 700 - 900°C	69

LIST OF ABBREVIATIONS

SEM	Scanning electron microscope
SMA	Shape memory alloy
VPSEM	Variable pressure scanning electron microscopy
EDS	Energy dispersive spectroscopy
DSC	Differential scanning calorimetry
QCA	Quench cooling accessories
TGA	Thermal gravimetric analysis
XPS	X-ray photoelectron spectroscopy
EFTEM	Energy-filtered transmission electron microscopy
HAADF	High-angle annular dark field
BSE	Back scattered electrons
VIM	Vacuum induction melting
PPM	Parts per million
HCP	Hexagonal cubic packing
FCC	Face centred cubic

LIST OF SYMBOLS

M_s	Martensite start
M_f	Martensite finish
A_s	Austenite start
A_f	Austenite finish
ΔH_f	Delta enthalpy formation
T	Temperature
t	time
K	Kelvin
$^{\circ}C$	Celsius
J	Joule
\AA	Angstrom
k'	parabolic constant
x	thickness

KESAN PERTUMBUHAN Ni_3Ti KE ATAS ANALISA PENGOKSIDAAN ALOI INGATAN BENTUK NiTi

ABSTRAK

Nikel – Titanium (NiTi) aloi ingatan bentuk telah mendapat populariti yang tinggi dalam implan dan peralatan perubatan sejak beberapa dekad yang lalu disebabkan oleh keserasian biologi aloi ini. Keserasian biologi ini dicapai dengan pembentukan lapisan nipis titanium dioxida (TiO_2) di permukaan hasil daripada proses pengoksidaan terkawal. Lapisan ini berkesan menghalang pelepasan nikel ke dalam tubuh manusia. Tindak balas pengoksidaan TiO_2 ini adalah kompleks dan kadar tindakbalas adalah sangat tinggi terutama pada suhu tinggi. Ia melibatkan pembentukan Ni_3Ti dan larutan pepejal $\text{Ni}_n(\text{Ti})$ apabila tempoh pengoksidaan dipanjangkan. Kajian ini mengukur kadar pembentukan ketebalan Ni_3Ti untuk mengkaji hubungan pembentukan TiO_2 terhadap variasi suhu dan masa. Sampel aloi diletakkan pada suhu 700 - 900°C pada jangka masa yang berbeza (10 – 200 minit) di dalam persekitaran udara. Didapati bahawa pertumbuhan lapisan Ni_3Ti pada 900°C adalah parabola dan mencapai ketepuan kira-kira 4 μm selepas 60 minit. Pada 700°C, lapisan mencapai ketepuan pada ketebalan kira-kira 1 μm selepas 60 minit. Pada keadaan yang melampau (pada suhu 900°C selama 200 minit) pertumbuhan ketebalan kekal stabil pada ~ 3.5 - 4.0 μm walaupun selepas pengoksidaan dipanjangkan tempohnya. Keputusan Analisis Termogravimetri (TGA) yang dijalankan pada kondisi eksperimen yang sama telah menunjukkan bahawa tingkah laku pertumbuhan TiO_2 adalah faktor penentu pertumbuhan lapisan Ni_3Ti dan lapisan TiO_2 juga memperlihatkan pertumbuhan parabola. Kalorimeter Pengimbasan

Perbezaan (DSC) pengukuran juga menunjukkan bahawa suhu transformasi NiTi mengalami perubahan yang ketara pada suhu 900°C dan 800°C manakala pada suhu 700°C kelakuan transformasi martensit dilihat stabil. Saiz puncak transformasi pula dilihat menurun pada suhu 900°C dan 800°C dengan peningkatan ketebalan Ni₃Ti.

EFFECT OF Ni_3Ti FORMATION ON THE OXIDATION KINETICS OF NiTi SHAPE MEMORY ALLOYS

ABSTRACT

Nickel - Titanium (NiTi) shape memory alloys have gained its popularity in many medical implants and their apparatus for the past few decades owing to their excellent biocompatibility. This attribute is achieved by the formation of thin layer of titanium dioxide (TiO_2) at the surface from a controlled oxidation process. This layer effectively hinders nickel release into the human body. Oxidation reaction of TiO_2 is complex and the reaction rate is very high especially at elevated temperature. It involves the formation of Ni_3Ti and solid solution $\text{Ni}_n(\text{Ti})$ as the oxidation prolongs. This work quantifies the rate of Ni_3Ti formation thickness for establishing a relation in controlling the thickness growth of TiO_2 with respect to temperature and time variations. The alloy was subjected to heat treatment at $700 - 900^\circ\text{C}$ for various times (10 – 200 minutes) in air environment. It was found that the growth of Ni_3Ti layer at 900°C is parabolic and reached saturation at thickness of about $4\text{ }\mu\text{m}$ after 60 minutes. While at 700°C , the layer reached saturation at thickness of about $1\text{ }\mu\text{m}$ after 60 minutes. At the extreme condition (900°C for 200 minutes) the thickness growth remained stable at $\sim 3.5 - 4.0\text{ }\mu\text{m}$ although after excessive oxidation treatment. Thermogravimetric Analysis (TGA) results that were ran under same oxidation conditions ($700 - 900^\circ\text{C}$ in air at same treatment time) has shown that the TiO_2 growth behaviour is the determining factor for the Ni_3Ti layer and it exhibited parabolic behaviour. Differential Scanning Calorimetry (DSC) measurements also indicated that the transformation temperatures of the NiTi alloy is altered

significantly at 900°C and 800°C while it is seen maintained at 700°C. The size of the transformation peaks is seen decreased with increasing Ni₃Ti thickness at 900°C and 800°C.

ACKNOWLEDGEMENT

In the name of Allah, Most Merciful, Most Gracious, Alhamdulillah, I thank to God for His Help and Bless, finally I have come to this end.

This research project would not have been possible without the support of many personnel. I would like to express my gratitude to my superb sporting supervisor, Dr. Abdul Rahim Othman who was abundantly helpful and offered invaluable assistance, support and guidance. Deepest gratitude is also due to the member of the supervisory committee, Professor Dr. Hazizan Md Akil from School of Material and Mineral Resources Engineering. Also, I am deeply grateful and sincere thanks to all of the technicians involve in completing my research including they are from School of Material and Mineral Resources, Aerospace and needless to mention, School of Mechanical Engineering.

During this work, special thanks to all my beloved friends, seniors and juniors who always had been there whenever I needed help. Not forgetting, my warm thanks to few of my special friends who always supporting me as my back bone, and never gave me untiring help during my difficult moments. In addition, I would like to express my deepest gratitude to my sponsorship. As one of the RLKA scholar, appreciation is given to Kementerian Pengajian Tinggi (KPT) and Universiti Sains Malaysia as being my financial aid throughout my studies.

I owe my loving thanks to my beloved parents, Mr. Amir Idris and Madam Rohayami Mohamad. Without their encouragement and understanding, it would have been impossible for me to finish this work. My special gratitude is due to my brothers and my sister for their loving support, understanding and endless love,

through the duration of my studies. Lastly, I offer my regards and blessings to all of those who supported me in any respect during the completion of the project.

TABLES OF CONTENTS

ACKNOWLEDGEMENT	ii
TABLE OF CONTENTS	iv
LIST OF TABLES	viii
LIST OF FIGURES	x
LIST OF SYMBOLS AND ABBREVIATION	xvi
ABSTRAK	xvii
ABSTRACT	xix

CHAPTER 1 – INTRODUCTION

1.1	Honeycomb Sandwich Structure.....	1
1.2	Impact Characteristic of Sandwich Structure.....	3
1.3	Energy Absorption and Failure Mechanism.....	4
1.4	Problem Statement.....	6
1.5	Aim and Objective.....	8
1.6	Thesis Structure.....	12

CHAPTER 2 – LITERATURE REVIEW

2.0	Introduction.....	13
2.1	Material Constituent.....	13
2.1.2	Composite Laminate.....	13
2.1.2	Thermoplastic Honeycomb Core.....	14
2.2	Sandwich Structure / Concept Design.....	16
2.3	Mechanical Property Tests for Laminates and Sandwich Structures.....	20
2.3.1	Compression Test.....	20
2.3.2	Flexural Test.....	21

2.3.3	Indentation Test.....	22
2.3.4	Tensile Test.....	24
2.3.5	Low Velocity Impact Test.....	25
2.3.6	Compression after Impact (CAI).....	26
2.4	Failure Analysis.....	27
2.4.1	Failure Behavior.....	28
2.4.2	Impact Response of the Laminates and Sandwich Structure.....	31
2.4.3	Impact Damage Resistance.....	34
2.4.4	Strength Reduction of Laminated Composite Structure	36
2.5	Energy Absorbed by the Sandwich Structure after Impact.....	38
2.5.1	Effect on the Thickness of Facesheet and Honeycomb.....	41
2.5.2	Energy Balance Model (EBM).....	43
2.6	Summary.....	44

CHAPTER 3 – METHODOLOGY

3.0	Introduction.....	46
3.1	Materials Preparation.....	46
3.1.1	Material Specification.....	46
3.1.2	Fabrication – Laminated Skin.....	48
3.1.3	Fabrication – Sandwich Structure.....	52
3.2	Mechanical Property Tests.....	53
3.2.1	Tensile Test.....	54
3.2.2	Edgewise Compressive Test.....	55
3.2.3	Flatwise Compressive Test.....	56
3.2.4	Three Point Flexural Test.....	58

3.2.5	Indentation Test.....	60
3.3	Low Velocity Drop Weight Impact Test.....	62
3.4	Compression after Impact (CAI).....	65
3.5	Optical Surfaces Metrology.....	65
3.6	Energy Balance Model.....	66
3.7	Summary.....	68

CHAPTER 4 – RESULTS & DISCUSSION

4.1	Introduction.....	69
4.2	Mechanical Property Characteristic of Thermoplastic Sandwich Composite	70
4.2.1	Tensile and Compression Properties of Composite Skin.....	70
4.2.2	Compressive Properties of Composite Sandwich.....	73
4.3	Low Velocity Impact Response.....	78
4.4	Effect of Compression after Impact on the Strength Reduction.....	80
4.5	Energy Absorption Characteristic of Thermoplastic Sandwich Composite...	85
4.6	Energy Balance Model (EBM) in Characterizing Impact Properties of Thermoplastic Sandwich Composite.....	88
4.6.1	Contact Effect from Indentation.....	88
4.6.2	Bending and Shear Effect through Flexural.....	94
4.6.3	Effect of Impact Force in EBM through Low Velocity Impact.....	99
4.6.4	Energy Dissipation Characteristics of Thermoplastic Sandwich Composite.....	103
4.7	Failure Analysis on Thermoplastic Composite Laminate and Sandwich....	108
4.7.1	Skin Failure Analysis.....	108
4.7.2	Polypropylene and Polycarbonate Honeycomb Core Crushing.....	112
4.7.3	Failure Mode Map.....	116

4.8	Summary.....	121
-----	--------------	-----

CHAPTER 5 – CONCLUSION

5.1	Conclusion.....	125
-----	-----------------	-----

5.2	Future Work.....	127
-----	------------------	-----

REFERENCES.....	128
------------------------	------------

APPENDIX A.....	136
------------------------	------------

LIST OF PUBLICATION.....	137
---------------------------------	------------

LIST OF TABLES

	Page
Table 2.1 HONYLITE™ Polycarbonate honeycomb uses include wind tunnels - grilles, sandwich cores, radomes - antennae, skylights, energy absorbing structures and EMI/RFI shielding.	16
Table 3.1 Material specification.	47
Table 3.2 Adhesive physical properties.	47
Table 3.3 Mechanical properties for Epolam 2025.	48
Table 3.4 Purpose and the function of each item needed for vacuum bagging process.	49
Table 3.5 Cured properties of Epolam 2025.	52
Table 3.6 Testing parameters.	64
Table 4.1 Mechanical properties for polypropylene sandwich Structure.	76
Table 4.2 Strength reduction of PP and PC sandwich structure undergoing compression after impact.	84
Table 4.3 Comparison of theoretical and experimental maximum force which shown the EBM id predicted for GFR laminate.	100
Table 4.4 Percentage of energy dissipation for GFR laminates	103
Table 4.5 Percentage of energy dissipation for PP and PC honeycomb sandwich structure for core thickness of 10mm.	104
Table 4.6 Percentage of energy dissipation for PP and PC honeycomb sandwich structure for core thickness of	

	30mm.	105
Table 4.7	Percentage of energy dissipation for PP and PC honeycomb sandwich structure for core thickness of 60mm.	106
Table 4.8	Indentation depth of PC and PP thermoplastic honeycomb sandwich structure based on 2D and 3D infinite focus surfaces metrology Alicona.	112
Table 4.9	2D and 3D failure images for GRP taken from infinite focus surfaces metrology Alicona.	114
Table 4.10	Polypropylene (PP) (left) and Polycarbonate (PC) (right) core crushing result analysis.	117

LIST OF FIGURES

		Page
Figure 1.1	Summarize the methodological frame work of the study presented in this thesis.	10
Figure 2.1	Sectional texture of a honeycomb-like cell.	15
Figure 2.2	Polycarbonate honeycomb exhibits a unique cell structure.	15
Figure 2.3	Composition of a polypropylene sandwich structure.	18
Figure 2.4	Sample construction setup.	19
Figure 2.5	Force-deflection schematic for the sandwich beam. (i)Upper skin compression failure, (ii) core crushing, (iii) lower skin tensile failure	30
Figure 2.6	Diagram illustrating post-impact core damage.	32
Figure 2.7	Existing design panels with varies core thickness.	42
Figure 3.1	Schematic diagram of material arrangement.	47
Figure 3.2	Schematic diagram of vacuum bagging process for laminate.	49
Figure 3.3	Sequence of fabricating the laminates.	51
Figure 3.4	The equipment used for the sandwich panel construction. (Left-right) Sheet metal cutter, hydraulic hot press and potable circular saw.	53
Figure 3.5	Instron Table Mounted Universal testing Machine (UTM).	54

Figure 3.6	Diagram of sample for tensile (length: 21cm) test and compression (length: 7.5cm) test.	55
Figure 3.7	Schematic diagram of edgewise compression test setup.	56
Figure 3.8	Close-up of specimen set up for flatwise compression test.	57
Figure 3.9	Diagram of sample for flexural testing arrangement.	58
Figure 3.10	Schematic plot of δ/PL against L^2 .	59
Figure 3.11	Schematic outlining how the contact parameters were determined following the indentation tests.	61
Figure 3.12	Indentation test setup.	62
Figure 3.13	Dimension of the drop weight impact testing sample.	63
Figure 3.14	Schematic diagram of drop weight impact tower.	64
Figure 3.15	Infinite Focus Alicona.	66
Figure 4.1	Sequence of failure during edgewise compressive test.	70
Figure 4.2	Images of failure due edgewise compressive test.	71
Figure 4.3	Typical stress versus strain curves undergo edgewise laminates compression test.	71
Figure 4.4	Images of tensile test result.	72
Figure 4.5	Typical stress strain curves for tensile laminates testing.	72
Figure 4.6	Different of thickness with core crushing effect after	

	flatwise compression tests.	74
Figure 4.7	Typical compression curves for Polypropylene honeycomb sandwich with three different core thicknesses.	75
Figure 4.8	Typical compression stress versus strain curves of Polycarbonate honeycomb with three different thicknesses.	75
Figure 4.9	Typical compression stress versus strain curves of Polypropylene honeycomb with three different thicknesses.	76
Figure 4.10	Sequences taken from the high speed video camera.	78
Figure 4.11	Typical load versus time curves for polypropylene honeycomb core subjected to 20J impact load for three different thicknesses.	78
Figure 4.12	Typical curves of compression extension versus core Thickness for polypropylene honeycomb sandwich.	81
Figure 4.13	Typical curves of compression stress versus core thickness for polypropylene honeycomb sandwich.	81
Figure 4.14	Load versus Displacement curves for 10mm core thickness of polypropylene sandwich undergoes compression after impact.	82
Figure 4.15	Energy absorption for GFR laminates.	86
Figure 4.16(a)	Energy absorption for PC and PP honeycomb with core thickness of 10mm.	86
Figure 4.16(b)	Energy absorption for PC and PP honeycomb with core thickness of 30mm.	87
Figure 4.16(c)	Energy absorption for PC and PP honeycomb with core thickness of 60mm.	87

Figure 4.17 (a-c)	Three different thickness of polycarbonate (left) and polypropylene (right) sandwich after undergo indentation test. Images of a-c indicate three core thicknesses of 10, 30 and 60mm.	89
Figure 4.18(a)	Typical Load-indentation curves for Polycarbonate core with three different core thickness.	90
Figure 4.18(b)	Typical Load-indentation curves for Polypropylene core with three different core thicknesses.	90
Figure 4.19(a)	A logarithmic plot of force against indentation for Polycarbonate Honeycomb core showing the curve fitting method for determining the indentation parameters ' n ' and ' C ' used in Meyer's law.	91
Figure 4.19(b)	A logarithmic plot of force against indentation for Polypropylene Honeycomb core showing the curve fitting method for determining the indentation parameters ' n ' and ' C ' used in Meyer's law.	92
Figure 4.20	The variation of the contact parameter ' n ' for Polypropylene and Polycarbonate core with different Thickness.	93
Figure 4.21	The variation of the contact parameter ' C ' for Polypropylene core with different thickness.	93
Figure 4.22	Position during carried out three point bending test.	94
Figure 4.23	Images of failure due to three point bending test for GRP laminates with five different span lengths.	95
Figure 4.24 (a-c)	Images of failure due to three point bending test for three different thickness of polypropylene with five different span lengths.	95

Figure 4.25	Load-Displacement plot of polycarbonate and polypropylene sandwich structure with 30mm core thickness and 150mm span length subjected to three point bending test.	97
Figure 4.26	Determination of the shear modulus, G and bending stiffness, D for Polypropylene with 10mm of core thickness using the method described in chapter 3.	97
Figure 4.27	The variation of shear modulus of the polypropylene and polycarbonate honeycomb with different thicknesses.	98
Figure 4.28	The variation of the maximum impact force with impact energy for GFR epoxy laminate.	99
Figure 4.29	The variation of the maximum impact force with impact energy for Polycarbonate and Polypropylene 10mm thickness.	101
Figure 4.30	The variation of the maximum impact force with impact energy for Polycarbonate and Polypropylene 30mm thickness.	101
Figure 4.31	The variation of the maximum impact force with impact energy for Polycarbonate and Polypropylene 60mm thickness.	102
Figure 4.32	Energy breakdown during impact on GFR laminates.	103
Figure 4.33(a)	Energy breakdown during impact on polycarbonate and polypropylene honeycomb sandwich structure for core thickness of 10mm.	104
Figure 4.33(b)	Energy breakdown during impact on polycarbonate and polypropylene honeycomb sandwich structure for core thickness of 30mm.	105

Figure 4.33(c)	Energy breakdown during impact on polycarbonate and polypropylene honeycomb sandwich structure for core thickness of 60mm.	106
Figure 4.34(a)	Variation percentage of energy dissipation for polycarbonate honeycomb for different core thickness.	107
Figure 4.34(b)	Variation percentage of energy dissipation for polypropylene honeycomb for different core thickness.	107
Figure 4.35	Typical honeycomb core crush curve.	115
Figure 4.36	Failure modes map in the quasi static experiments based on the relationship of displacement and core thickness.	121
Figure 4.37	Failure modes map in the quasi static experiments based on the relationship of critical load and core thickness.	122

LIST OF SYMBOLS AND ABBREVIATION

m	meter
mm	millimeter
mm ²	square millimeter
in ²	square inch
kN	kilo Newton
J	Joule
J/m ²	Joule per meter square
atm	atmosphere
psi	pound per square inch
°C	Degree Celcius
2D	Two Dimensional
3D	Three Dimensional
PP	PolyPropylene
PC	PolyCarbonate
FRP	Fibre-Reinforced Plastic
GFRP	Glass Fibre Reinforced Polymer
CFRP	Carbon Fibre Reinforced Polymer
SMC	Sheet Moulding Compound
GMT	Glass Mat Thermoplastic
BVID	Barely Visible Impact Damage
ASTM	American Standard Testing Material
EF	Elastomeric Foam
PUR	Polyurethane

PENCIRIAN MEKANIKAL DAN KEGAGALAN KOMPOSIT

TERMOPLASTIK *SANDWICH* SARANG LEBAH

ABSTRAK

Kajian ini menumpukan kepada kegagalan / kerosakan dan penyerapan tenaga bagi konstituen bahan termoplastik berstruktur *sandwich* sarang lebah dengan tiga teras yang berbeza ketebalan 10, 30 dan 60 mm. Tumpuan kajian diberi dalam memfabrikasi komposit kulit berlapis, termoplastik berteras sarang lebah polipropilena (PP) dan polikarbonat (PC) yang dilakukan dalam ujian hentaman berhalaju rendah pada tenaga hentaman 20, 60, 120 J. Kaedah pematangan komposit laminat 5 lapisan kulit E gentian kaca dengan orientasi $[0/90/\pm 45/0/90]$ disediakan menggunakan pembalut vakum dengan kerjasama pihak industri, AMRED Sirim Berhad, Kulim. Satu siri ujian pencirian yang berkaitan dengan kulit komposit telah dijalankan seperti, ujian mampatan, ujian tegangan dan ujian lenturan tiga titik dengan kadar sensitiviti 1 mm/min. Kajian terhadap struktur komposit *sandwich* juga melibatkan analisis mikrostruktur dalam mengenalpasti kerosakan setempat dan kerosakan keseluruhan kekuatan struktur / bahan yang disebabkan kesan hentaman jatuh bebas. Kuantifikasi kapasiti penyerapan tenaga bahan komposit akan ditentukan melalui mod kegagalan yang berbeza dengan menggunakan model pengkomputeran imbalan tenaga bagi pengoptimuman reka bentuk struktur. Selain daripada ujian hentaman berhalaju rendah, ujian lenturan tiga titik dan ujian lekukan akan dijalankan secara serentak bagi mendapatkan model keseimbangan tenaga, dan pada masa yang sama tenaga nyahserapan oleh lentur / ricih dan sentuhan juga boleh ditentukan. Buat kali pertama, model imbalan tenaga dilanjutkan untuk meramalkan pembahagian tenaga untuk memahami bagaimana tenaga penghentam

yang dikenakan diserap secara dinamik oleh struktur *sandwich*. Oleh itu, penambahbaikan struktur bahan yang menyumbang kepada peningkatan prestasi dapat dilakukan dengan memperkenalkan peta mod kegagalan dan pengiktirafan kegagalan untuk bahan termaju komposit mengikut faktor kerosakan dan tahap tenaga. Di samping itu, mampatan selepas perlanggaran (CAI) dijalankan untuk menentukan pengurangan kekuatan struktur *sandwich*. Sebagai kesimpulan daripada kajian ini, tenaga diserap dan tenaga yang dilesapkan oleh laminat dan struktur *sandwich* diperolehi. Selain perbandingan antara kekuatan dan kekakuan bahan, pencirian kegagalan diperolehi juga.

MECHANICAL AND FAILURE CHARACTERIZATION OF THERMOPLASTIC HONEYCOMB SANDWICH COMPOSITE

ABSTRACT

This research focusing on failure/damage response and energy absorption on different constituent material of thermoplastic honeycomb sandwich structure with three different core thicknesses of 10, 30 and 60 mm. In this present investigation, the interest will be on the fabrication of laminated composites skin, polypropylene (PP) and polycarbonate (PC) thermoplastic honeycomb core subjected to low velocity impact test of impacted energy 20, 60, 120 J. Curing method of the composite laminates of 5 layers E-glass fiber with orientation $[0/90/\pm 45/0/90]$ by using vacuum bagging is used with collaboration with the industry, AMREC Sirim Berhad, Kulim. Relevant properties of the composite skin was measured by conducting a series of properties test, such as, compression test, tensile test and three point bending test with rate sensitivity of 1 mm/min. This research of the composite sandwich structure also included identification on the localized damage and globalised damage on the structural / material integrity due to the drop weight impact through microstructure analysis. Quantification of the energy absorption capacity of the composite materials will be determined through different failure mode by computing energy-balance model for structural design optimization. In order to obtain the energy-balance model, other than low velocity impact test, three point flexural tests and indentation test will be carried out concurrently, energy dissipation by bending/shear and contact can also be determined. For the first time, the energy-balance model is extended to predict energy partitioning in order to understand how the energy of the impactor is absorbed by the dynamically loaded sandwich structure. Thus, improved structural materials can contribute to improved performance by

introducing the failure mode map and failure recognition for advanced composite material according to the damage factor and energy level. In addition, compression after impact (CAI) is carried out to determine the strength reduction of the sandwich structure. As a conclusion from this study, energy absorbed and energy dissipated by the laminates and sandwich structure are obtained. Besides comparison between the toughness and stiffness of the materials, failure characterization is obtained as well.

CHAPTER 1: INTRODUCTION

1.1 Honeycomb Sandwich Structure

Structural sandwich composite panels are nowadays widely used in aerospace, marine, automotive, locomotive, windmills, building consumer industries due to their excellent properties like superior bending stiffness, low weight, excellent thermal insulation and acoustic damping, fire retardancy, ease of machining and ease of forming among others (Hosur et al.,2004). The American Standard for Testing Materials, ASTM, defines a sandwich structure as “a special form of a laminated composite comprising of a combination of different materials that are bonded to each other so as utilize the properties of each separate component to the structural advantage of the whole assembly”. The faces are usually thin and stiff in order to provide the required bending and shear stiffness and to carry the edgewise and bending loads as well as the in plane shear loading. The properties of the core vary depending on the application. However the main function of core material is to stabilize the facings and carry shear loads through the thickness. It should therefore be rigid and as light possible. Generally, three main elements needed for sandwich construction are:

- i. Two thin and strong sheets (skin)
- ii. A thick layer of low density material which may be less stiff and strong than the skins (core)
- iii. An adhesive joint to hold the skins and core in place to form a continuous structure

Today, sandwich structures are widely used in the fabrication of primary and secondary structures of civil and military aerospace components. The design

principle behind a sandwich structure is based on an I-beam, which is an efficient structural shape because much of the material is placed in the flanges situated farthest from the neutral axis. Only enough material is left in the connecting web to make the flanges act in concert and to resist shear and buckling loads. In a sandwich structure, the face takes the place of the flanges and the core takes the place of the web. The difference is that the core of a sandwich is of a different material from the faces and is as a continuous support for the faces rather than concentrated in narrow web in I-beam. Since the face and the core are of the different materials, an adhesive is used to bond these materials. The adhesive that is used to bond the faces to the core are therefore of critical importance.

According to history, a Frenchman called Duleau first discovered the concept of sandwich construction in 1820 as stated in (Zenkert,1995). Although the concept was discovered as early as this, it was only applied and made available commercially after one hundred years later. One of the earliest sandwich panels produced was an asbestos-faced sandwich panel with a fireboard core prior to World War Two. Another early application of sandwich construction was in the Mosquito aircraft produced in Britain in which part of the aircraft body was made of a balsa core sandwich panel with bonded Veneer faces. The development of high performance core materials started in the 1940s and efforts still continue in order to reduce the weight of engineering sandwich structures. Balsa was the first core material considered and used in the manufacture of cruising yachts and launches. Honeycomb core materials have appeared in the late 1940s and early 1950s and are currently used in many aerospace applications. Polymeric core materials such as polyvinyl chloride (PVC) and polyurethane (PU) appeared in the late 1950s and early 1960s. In addition, sandwich designs are also used in flooring, interior and exterior panels.

There are a variety of pleasure boats and ships made in sandwich design typically decks and hull structures. In civil engineering application, sandwich panels have been used for many years for their low weight and thermal insulation properties. In the aerospace, sandwich constructions have been used for manufacturing components such as wings, doors, control surfaces, radomes, tailplanes, stabilizers, space structures and antennae.

1.2 Impact Characteristic of Sandwich Structure

Low-velocity impact is defined as events in which, the upper limit of which can vary from 1 to 10 ms⁻¹ depending on the target stiffness, material properties and the impactor's mass and stiffness. In contrary, high-velocity impact response is dominated by stress wave propagation through the material, in which the time to respond of the structure was ignored, leading to much localized damage (Richardson and Wisheart,1996). Low velocity impact is considered potentially dangerous mainly because the damage might be left undetected, as the surface may appear to be undamaged (Othman and Barton,2008). A major concern that limits the usage of sandwich composites is their susceptibility to damage due to impact loading. There are practical situations such as tool drops, runway debris, bird strikes, hailstorms and ballistic loading, which could induce considerable damages to the composite structures.

As stated earlier, composites offer many advantages over traditional materials when specific properties are considered. However, composite materials do suffer from a number of limitations. The major limitation associated with composite

materials is their poor impact resistance. Laminated and sandwich composites are more susceptible to impact damage than similar metallic structures. Furthermore, the damage induced by the impact event is often visually undetectable and it may grow under subsequent loadings. This damage causes a reduction in strength and reduces the structures integrity. For low intermediate incident energies in composites, the ability to undergo plastic deformation is extremely limited with the result that energy is frequently absorbed in creating large areas of fracture with ensuing reductions in both strength and stiffness. The problem of poor impact resistance coupled with other problems often prevents composites from being used in aerospace and other applications. In order to maintain the durability and reliability of composites for these applications, the impact problem needs to be studied and investigated so that its effects can be controlled and minimized.

1.3 Energy Absorption and Failure Mechanism

The current generation of sandwich structures primarily utilizes foam, balsa and honeycomb as core materials. They offer great potential energy absorption and increase the flexural inertia without significant weight penalties. Energy absorption capabilities of the sandwich panels are highly inter-related with the velocity of impact. In addition, energy absorbed during impact is mainly dissipated by a combination of matrix damage, fiber fracture and fiber-matrix debonding in the face sheets, core crushing and face sheet-core debonding (Bhuiyan et al.,2009). One of the main drawbacks of these high performance sandwich structures, however, is its poor resistance to impact where damage resistance refers to the amount of impact damage which is induced in a composite system (Bhuiyan et al.,2009, Kang et al.,2008). In addition, unidirectional composite laminates are highly susceptible to the transverse impact loads resulting in significant damages such as matrix cracks,

delaminations, and fiber fracture (Aktas et al.,2009, Choi,2006). Delaminations, fiber breakage, and matrix cracks occur in the composite structure which depends on the impact parameters and material properties of the composites. Thus, evolvments of the composite structures have been investigated for better quality for application purposes (Ning et al.,2007).

Damage behavior and strength reduction of sandwich structure due to impact is greatly governed by both the material properties of core and stiffness and their thickness (Hosur et al.,2008, Kang et al.,2008, Park et al.,2008). By varying the core, the thickness and the material of the face sheet of the sandwich structures, it is possible to obtain various properties and desired performance (Shahdin et al.,2009). In contrast, composites can fail in a wide variety of modes and contain barely visible impact damage (BVID) which nevertheless severely reduces the structural integrity of the component.

It is sometimes difficult to get a clear insight into the fundamental phenomena occurring in response to loads. Thus, sequence in impact damage of sandwich composite is difficult to interpret because of the complexity involved. Such intricacy in experimental studies leads to the growing need for analytical and/or finite element solutions, especially during preliminary analysis prior to final configuration design. Such studies provide valuable information particularly on the damage magnitude and sequence as well as establishing design criteria. Solutions that can provide good estimations of load-bearing capacity and damage mechanisms enable important parameters to be identified. Numerical analysis can therefore provide further clarification of the structural behavior and failure mechanisms of sandwich composites with respect to the parameter variations. As a result, a number

of studies have been carried out to help the understanding and improve the impact response and failure analysis of composite material and sandwich structures.

1.4 Problem Statement

Since the first days of powered flight, aircraft designers have focused on achieving minimum weight. Therefore, composite materials were used in the making of most of the aircraft parts. However, choosing the correct honeycomb core for application purposes can be very difficult problem. Not only are there mechanical property, strengths and moduli requirements, but the environmental issues must also be considered: temperature exposure, moisture, water migration, relative humidity, fluids soak resistance, damage tolerance, impact resistance, etc (Bitzer,1997).

However, there is one major concern in the use of monolithic and sandwich composite material, which is the damage induced in these materials due to impact by foreign objects during their life span. Impact loading on a sandwich structure could lead to the localized damage which can lead to reduction in its load-bearing properties. Furthermore, impact may come from a variety of causes. Typically, low-velocity impact may result from tool drops, hail and debris thrown up from runways. In addition, the effect of low-velocity impact is of special concern in a variety of layered configurations.

A number of studies have focused on low-velocity impact responses of sandwich laminated structures. To understand the impact damage and strength reduction of sandwich structures, researches have focused on the energy-absorbing

capacity and on the residual core strength in impacted systems and indicated that the impact damage is easily affected by constituent materials (Kang et al.,2008, Aktas et al.,2009, Hazizan and Cantwell,2003). Also, due to the inertia effect, a beam under transverse impact will experience larger shear stress than that under quasi static loading. Hazizan and Cantwell (2003) have conducted low velocity drop weight impact tests on the glass fibre/epoxy aluminium honeycomb sandwich structures. They developed and found that a simple energy-balance model (EBM) based on the dissipation of the incident energy of the projectile during the impact event which involve bending, shear and contact effect deformation can be used to predict the energy absorption capacity of aluminium honeycomb sandwich structure. Thus, the model is useful and will be used to quantify the energy absorption of the sandwich structure in this study.

Furthermore, failure behavior of composite laminates and sandwich structure has been investigated by several researchers. By considering the energy profile diagrams and associated load-deflection curves on impact response of unidirectional glass/epoxy laminates, at lower impact energies, the main damage mode was found as delamination and matrix cracks (Aktas et al.,2009). However, for the higher impact energies, fiber failures were dominant due to the brittle characteristics of glass fabrics (Aktas et al.,2009). Significant delaminations were observed at the bottom layers, resulting from vertical displacement of the broken and unbroken fibers at point of impact rather than the bending mismatching. Studies on indentation failure behavior of honeycomb core sandwich panels by examining the effects of skin, core and indenter size on load transfer from the top skin to the core was proven

by analytical solutions. Examination on the mechanical properties and failure mechanism leads to the contribution on the development of the failure mode map.

Nonetheless, impact behavior of sandwich structures is apparently still a problem need to be further investigated. In this present investigation, the interest will be on the fabrication of laminated composites skin, polypropylene (PP) and polycarbonate (PC) thermoplastic honeycomb core and damage/failure investigation. Varieties of parameters are included for the sandwich structures damage/failure investigation purposes such as impact energy, honeycomb core thickness and etc. The study also included investigation on the localized damage and energy absorption capacity of the composite materials which involve modification of energy-balance model, and also different failure behavior of the composite structure. For the first time, the energy-balance model is extended to predict energy partitioning in order to understand how the energy of the impactor is absorbed by the dynamically loaded sandwich structure. Thus, improved structural materials can contribute to improved performance by introducing the failure mode map and failure recognition for advanced composite material.

1.5 Aim and Objective

The purpose of this research is to achieve certain aim such as:

- i. To quantify the energy absorption through different failure mode by computing energy model for structural design optimization.
- ii. To identify the effect of localized and globalised damage on the structural / material integrity through microstructure analysis.

- iii. To enumerate failure analysis on sandwich structure composite laminated panel and to develop failure mode map according to the damage factor and energy level.

The following figure summarizes the methodological frame work of the study presented in this thesis.

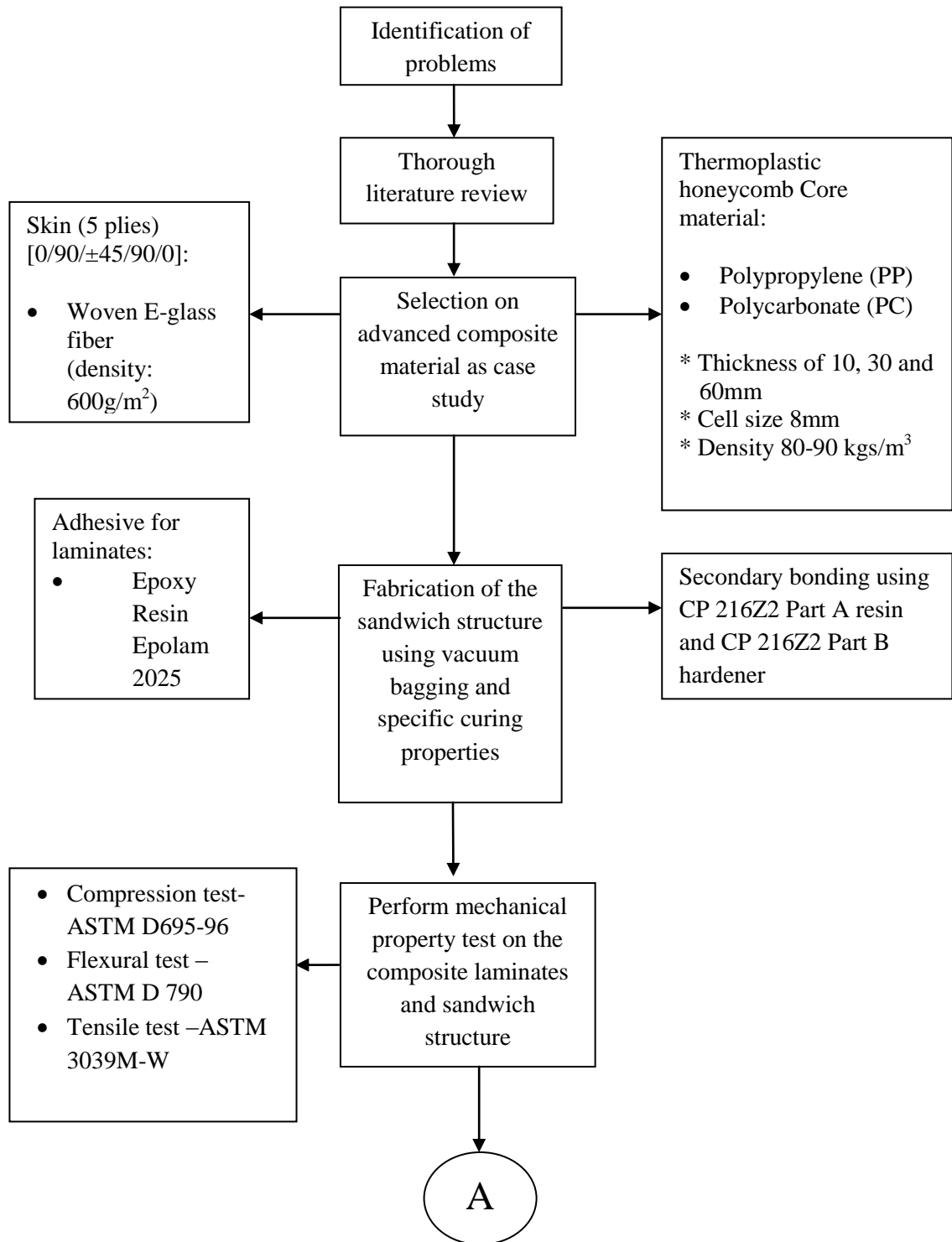
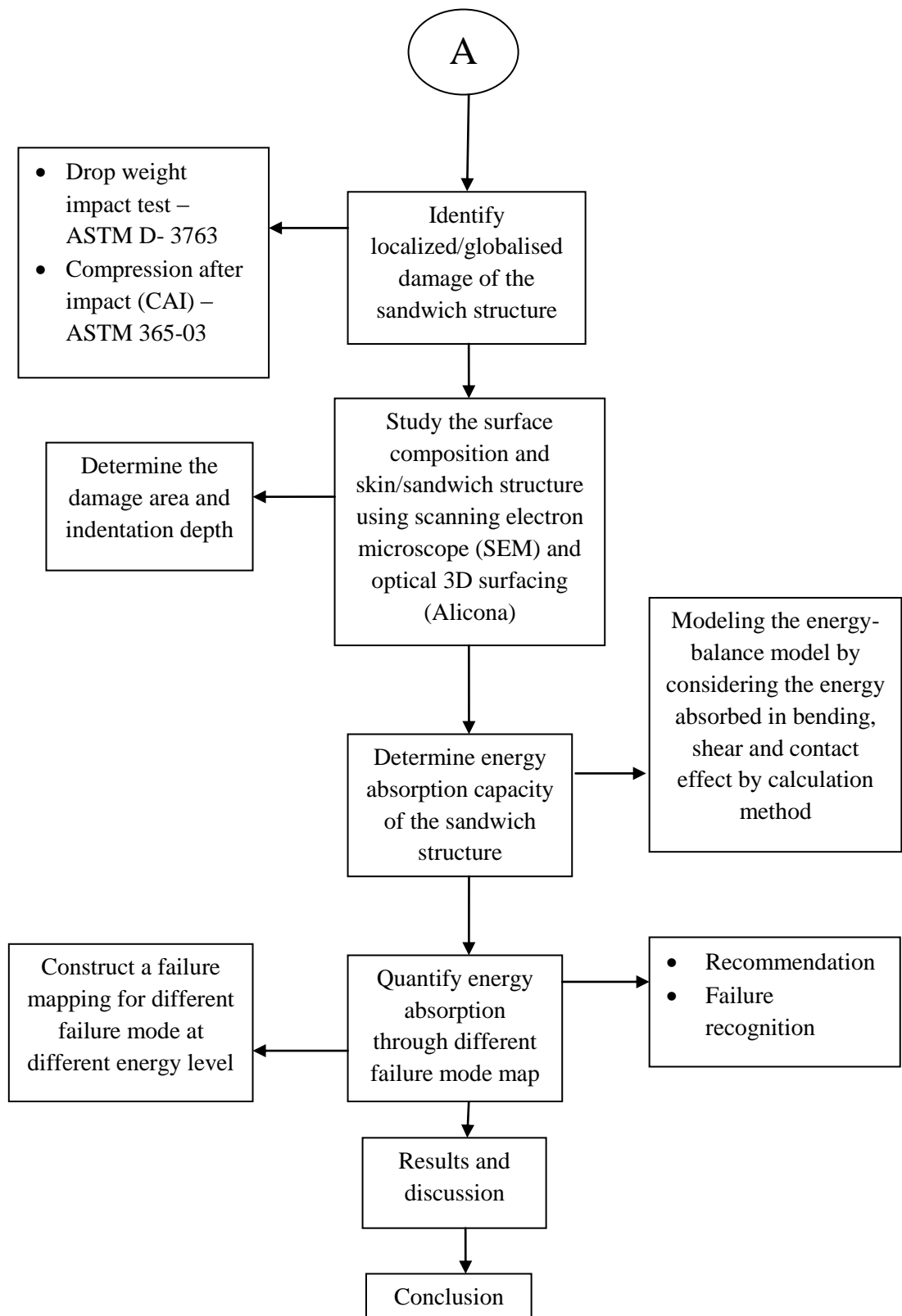


Figure 1.1 Summarize the methodological frame work of the study presented in this thesis.



1.6 Thesis Structure

This chapter has summarized the scope of work for this research and also the importance of the research specifically. The aim and objectives of the present work are stated clearly. The remaining chapters are organized as follows:

Chapter 2 contains extensive survey on related work presented by current researchers on composite sandwich structure subjected to low velocity impact and also the impact responses. Thus, thorough literature reviews for better understanding on current research are reviewed in this chapter.

Chapter 3 is focusing on the methodology of the research. Method of fabrication of the skin and the sandwich structure and also the experimental procedure that involve in this project will be explained in this chapter.

Analysis from the results of the experimental work obtained will be presented in chapter 4. Results from the experimental work concerning the facesheet material, sandwich structure, impact responses, residual strength, and cores thicknesses will be discussed. Comparison will be made by developing failure mapping regarding the damage types and also energy level involved. Exhaustive observation will be included based on the analysis performed.

Lastly, conclusion was made based on the results and discussion from the previous chapter. Key contributions of the whole research are stated clearly as well as future works required.

CHAPTER 2: LITERATURE REVIEW

2.0 Introduction

This chapter reviews recent advances in the development of composite sandwich in structural application. First, consideration is given on the properties of constituent materials, in which different materials and their advantages are discussed. Glass fiber reinforced polymers, have been used to replace traditional steel and aluminium components as lightweight composite materials (Ning et al.,2007). For example, more than 55% of the design feature of a sandwich composite with E-glass fiber/polypropylene (glass/PP) face sheets and PP honeycomb core has demonstrated good weight saving compared to conventional bus with aluminium skin and supporting steel bars (Ning et al.,2007). Also, different failure mechanisms and the effect of the loading rate, impact energy, thickness of the skin and core as well as the influence of geometrical configuration on the energy absorption are also reviewed.

2.1 Material Constituent

2.1.1 Composite Laminate

The most common reinforcing material in composites due to its superior strength/cost ratio is E-glass fiber (Ning et al.,2007). For instance, because GLARE (glass fibre reinforced epoxy/aluminium FML) has excellent fatigue and impact resistance and is commonly employed in commercial aircraft hulls, and has been proposed as a material for luggage containers (Fleischer,1996, Langdon et al.,2007). Certain experiments proved that woven textile sandwich panel has potential energy absorbing ability owing to its large plastic deformation capacity. In order to reveal the energy absorption capacity of the woven textile sandwich material and the failure mechanisms, quasi-static compression and three point bending tests were carried out.

The results show that the ideal material to serve as an energy absorbing core is woven textile sandwich (Fan et al.,2010).

Airbus 350 and Boeing 787 have used these composites in their primary structures. To manufacture structural components that are able to withstand extreme temperature in aeronautical and aerospace application, composite materials such as glass fiber, mainly carbon fiber/epoxy laminates, are vastly used. A primary aeronautical structure made of carbon fibre reinforced plastics (CFRP) has the ability to stand the assigned loads when a realistic distribution of barely visible impact damages (BVID) is present whose main factor is the core thickness (Richardson and Wisheart,1996, Park et al.,2008, Caprino et al.,2003). Typically, under impact loads, laminated composite materials in modern aircraft structures are not unloaded but under a certain state of prestress. Jawaid et al (2010) morphological study of impact fracture surfaces was investigated on the effect of fiber-matrix bonding and breakage of the composite with the help of scanning electron microscope (SEM).

2.1.2 Thermoplastic Honeycomb Core

Honeycomb is well known as an excellent absorber of impact energy. Besant et al (2001) proved that through thickness shear yielding and by a combination of local core crush under the impactor, honeycomb absorbs energy. On the other hand, cost-effective material and processing approaches applies for thermoplastic composite technologies. In addition, superior resistance to corrosion, high durability, low maintenance, easy replacement, impact damage tolerance, and modularity are the advantages of using thermoplastic (Ning et al.,2007).

Structures of high strength-to-weight ratio are highly desirable in the aerospace industry. For this reason, honeycomb sandwich structures are often made

out as airplane structural components. These sandwich structures consist of thin high-strength skins bonded on the top and bottom of a honeycomb core (Buehler and Seferis,2000). According to Gu (2000) a two dimensional glass fabric is used in order to compare properties between the laminated and integrated honeycomb-like cells (Figure 2.1). From the result obtained, a better anti-shearing performance was observed from integrated honeycomb-like structure. This is attributed to layers in the composite that are connected by filaments which in the laminated honeycomb-like cells case the resin bears the shearing stress. This is due to composite with a high volume fraction and high processing temperature window ($>30^{\circ}\text{C}$). Moreover, to manufacture sandwich structures, PP tubular honeycombs and rigid PP foam were also being used.

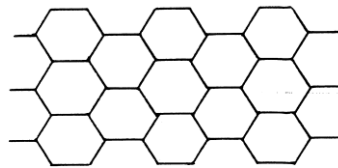


Figure 2.1 Sectional texture of a honeycomb-like cell.

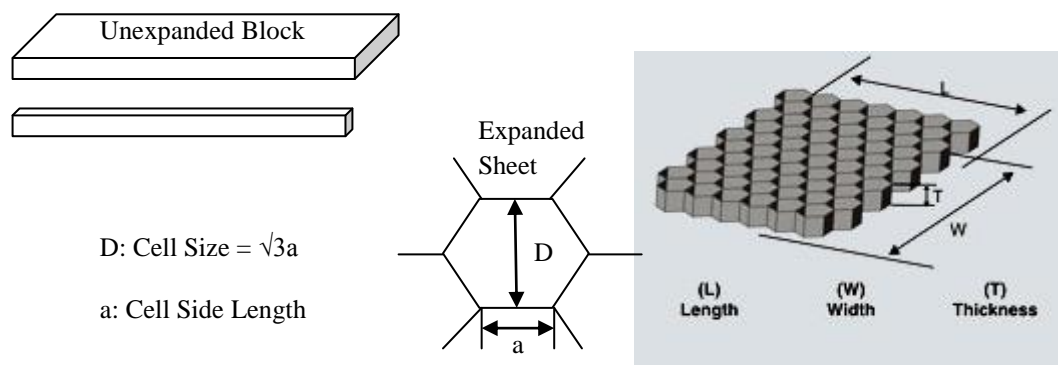


Figure 2.2 Polycarbonate honeycomb exhibits a unique cell structure (Gu,2000).

In Figure 2.2, some unique features possess by polycarbonate honeycomb core are good thermal and electric insulator, fire resistant, excellent dielectric properties, corrosion resistant, conductive grades available, sandwich skins can be melted to core, fungi resistant, small cell sizes at high densities, use temperature below 93°C (refer Table 2.1), and last but not least available transparent and in colors. The core has 3 orientations in contrast to the 2 orientations as with the other honeycomb, which makes its properties more uniform. The tubular form in each cell makes it inherently more stable.

Table 2.1 HONYLITE™ Polycarbonate honeycomb uses include wind tunnels - grilles, sandwich cores, radomes - antennae, skylights, energy absorbing structures and EMI/RFI shielding.

PC2 Polycarbonate Mechanical Properties						
PLASCORE[®] Honeycomb Designation			Typical Bare Compressive		Typical Plate Shear	
CORE TYPE	CELL SIZE	DENSITY PCF	STRENGTH PSI	MODULUS KSI	STRENGTH PSI	MODULUS KSI
PC2	1/8	5.0	280	30	110	3.2
PC2	1/4	4.0	210	26	90	3.3

2.2 Sandwich Structure/ Concept Design

Sandwich panels are mostly utilized in manufacture of sports equipment, automotive and aeronautical structures. In general these sandwich panels are made up of three layers, in which a low density material separates the two thin sheets (faces) made of stiff and strong material (Anderson and Madenci,2000a). Therefore it is necessary to employ material of high quality in the core to obtain an optimal design. A new concept sandwich structure embedded with composite columns has been designed and manufactured by (J.L.,1992). These 3D sandwich structures with

foam were fabricated, tested and analyzed under bending, out-of-plane compressive and shear loadings. It was found that the interface of facesheets-to-foam core prevent the core from debonding and vertical composite columns from crushing. By using the design of the column foam sandwich structure, low strength and delamination between facesheet and core in the sandwich composite can be effectively overcome. It is clear that composite properties were mainly dependent on the properties of lignocellulosic fibers. Moreover, discussion on mechanical properties, failure modes, and design requirements of sandwich panels containing all-PP laminate faces (Figure 2.3) are compared with sandwich panels of different materials containing conventional glass fiber reinforced polypropylene laminate faces (Anderson and Madenci,2000a). In resulting the sandwich panels clearly contain no “foreign” reinforcements, all-PP laminates being used as the sandwich face panels, together with PP based hot melt adhesives and a PP based core (Anderson and Madenci,2000a).

Cabrera et al (2008) target the appropriate damage by described the design, manufacture and testing of a self-healing system for target damage. In the study of practical engineering sandwich structure, the vascular self-healing approach was developed for sandwich beams by applying the edgewise compression after impact test configuration. From this analysis, it was shown that self-healing system has several advantages in advanced structures. Thin laminated composite face sheets bonded to a relatively thick, compressible structural foam core layer are used in marine and ship structures. PUR interlayer resulting in reduction of both overall and local deflections of the face sheet, and also the residual stresses left after unloading and the local compression of the foam core. On the other hand, a much better

protection against compression of the foam core is offered by EF (elastomeric foam) interlayer. The residual stresses generated by foam core compression greatly reduce the strain energy release rates of interfacial cracks. It can be seen that the interlayers absorb most of its deflection, thereby decreasing the local core crushing by separating the core from the impacted sheet. Therefore, interface cracks are reduced substantially by the residual strains (Wang et al.,2010).

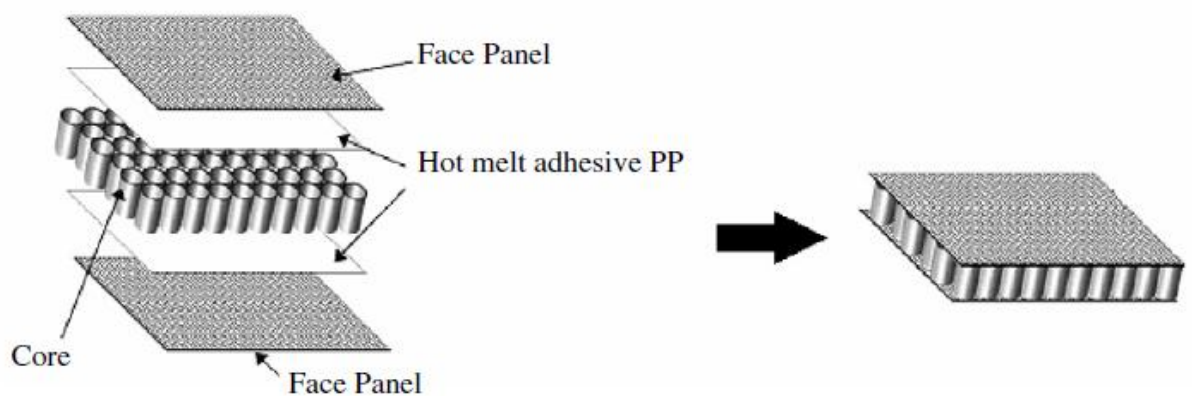


Figure 2.3 Composition of a polypropylene sandwich structure.

Furthermore, the fabrication of composite sandwich is affected by the type of epoxy resin used and it influences the absorption characteristics of the resultant composite (Buehler and Seferis,2000). According to Williams et al (2008) the damage in the resin-lean specimen takes place very near to the facesheet/honeycomb-core interface (Figure 2.4). Suvorov and Dvorak (2005) studied the delamination resistance affected by properties associated with the resin used. They investigated the properties of a various thermoset, toughened-thermoset and thermoplastic based composites. A double cantilever beam specimen was used in to order to evaluate the critical strain energy release rate.

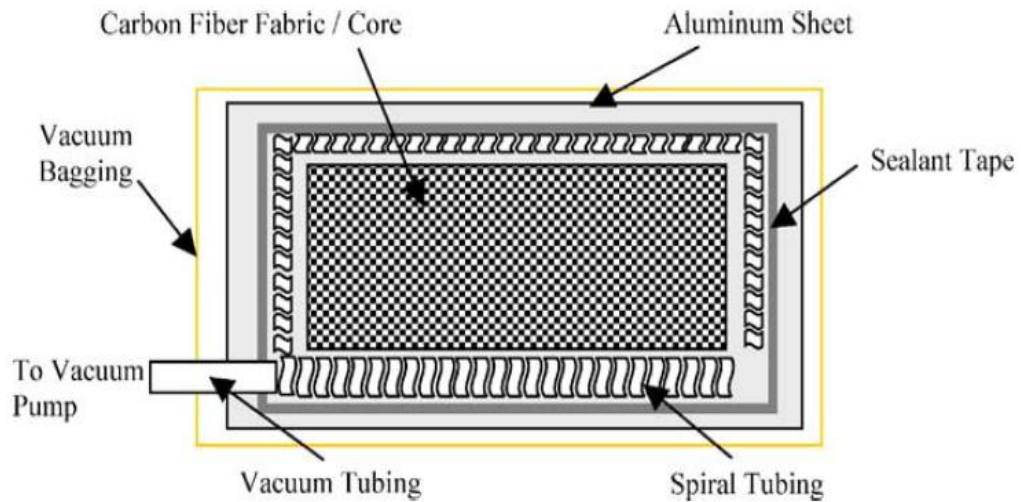


Figure 2.4 Sample construction setup (Sánchez-Sáez et al.,2008).

Following fracture tests on neat resins and their corresponding composite specimens, they identified a strong correlation between the critical strain energy release rate of the neat resin and the interlaminar fracture toughness, G_{Ic} of the associated composite (Buehler and Seferis,2000). A clear link between the properties of the matrix and those of the composite materials was observed for brittle polymers, here the value of G_{Ic} was slightly greater than the resin. For tough matrix resins, an increase of 3 J/m^2 in the resin G_{Ic} resulted in a 1 J/m^2 increase in the interlaminar fracture energy of the composite. For brittle resins, the interlaminar fracture toughness G_{Ic} is generally greater than the G_{Ic} of the neat resin values due to the fact that a full transfer of the neat resin toughness to the composite occurs. Furthermore, from the peel test evaluation, by varying parameters like copolymer film, nature of core material and temperature are varied, it is possible to optimize the bonding strength between the face and the core. Due to a higher surface contact area, it was shown that the foam-to-face bond was more homogeneous (Anderson and Madenci,2000a).

2.3 Mechanical Property Tests for Laminates and Sandwich Structures

2.3.1 Compression Test

Typically, compression tests comprise of an edgewise compressive test for laminates and a flatwise compressive test for sandwich structure. ASTM C 364-99 has been utilized as a standard test method to study edgewise compressive strength whereas for flatwise compressive properties of sandwich cores, ASTM C 365-03 is used. Using this method, the compression properties of a flat structural sandwich construction in a direction parallel to the sandwich facing plane can be evaluated. Also it is useful to determine the compressive strength and modulus of sandwich core. Even though the ASTM is used for the purpose of sandwich structure testing standard method; however it can be used as a reference for laminates testing method as well. Moreover, ASTM D 695-96, which is a standard test method to determine the compressive properties of rigid plastics, was also used as a reference for experimental purposes.

It may found that the retention factor at room temperature and a greater reduction of the residual strength is shown from compression after impact behavior (Kang et al.,2008). Since the reinforcement architecture limits crack propagation, it could also prevent the growth of delamination during compression tests (Chung et al.,2007). However, static compression tests of composite egg-box panel were carried out to investigate the various materials, deformation behavior and stacking sequence and number of plies on the energy absorption capacity (Kärger et al.,2008). The residual strength and residual stiffness are taken into account for core compression arises as the failure model (Ahmed and Vijayarangan,2008). Generally,

the compression induces shear deformation and densification becomes apparent in the later stage of compression (Fan et al.,2010).

2.3.2 Flexural Test

There are various ASTM standard test method available for the flexural testing, namely ASTM D 790-97, D 5147, D 638. These test methods are designed to suit both rigid and semirigid materials. This test comprises the evaluation of flexural properties of unreinforced and reinforced plastics that includes high-modulus composites materials cut from sheets, plates, or molded shapes or in the form of rectangular bars molded directly. However, materials that does not fail in the outer fibers within the 5% strain limit or do not break, cannot be used to determine the flexural strength in these test methods. A three-point loading system applied to a simply supported beam has been utilized in these test methods.

Mousa and Uddin (2009) made a considerable improvement in the flexural strength by arranging glass fiber plies as the top and bottom layers and jut fiber plies at the middle. For flexural specimen, no delamination between the jute and glass plies is noticed. As a result of the additional jute fiber layer, the flexural strength increased due to an increase in resistance to shearing (Jawaid et al.,2010). By using Tinius-Olsen Universal Testing Machine, strength and ductility responses were studied for panels under four point bending test (Jawaid et al.,2010). FRP laminates demonstrated significant influence on both strength and ductility of the FRP panels. To predict the strength of the FRP member, a theoretical analysis was carried out and good agreement with the experimental results were observed. The theoretical validity of the equations used in finding the flexural and shear capacities of FRP panels were justified by this method (Jiang and Shu,2005). For sandwich structure under three-

point-bending, the skin fracture dominates the thinner ones, whilst the skin crippling and shear failure influences the load capacity of the thicker panels. After the initial failure, the panels residual load capacity is rendered by the progression of plastic hinges in a long deflection plateau (Fan et al.,2010).

2.3.3 Indentation Test

A new model has been evaluated to predict the indentation as a function of indentation energy. It was observed that the constant appearing in it seem to be independent of the fibre architecture, laminate type, matrix type, and constraint conditions (Caprino et al.,2003). It was found that there are no major effect on the contact forces in the internal composite plies and the deflection of the sandwich structures, regardless of the impact energy and the locations of the internal ply (Sun and Chen,2010). Localized impact loading on composite structures will generate a localized deformation at the point of contact as a result of the contact between the impactor and the target. . In early studies (Bitzer,1997), local deformations were neglected as a result of assumption that the structures were inextensible in the transverse direction. Therefore, beam, plate or shell theories were not used to model local deformations in the contact zone. The gap between the displacement of the projectile and the back face of the structure is defined as the indentation. For most laminated composite materials, the contact response is recognized (Richardson and Wisheart,1996, Bitzer,1997) as being rate-independent and statistically-determined contact laws are used by many investigators. Contact law is defined as when the problem can be greatly simplified if the contact force is expressed as a function of the indentation. The behavior of the contact parameters, ' n ' and ' C ' in the Meyer

indentation law ($P=C\alpha^n$) need to be characterized over a range of loading conditions. The contact law for composites during the loading and unloading phases has been found to differ considerably even when the loading curve follows a linear Hertzian Contact Law. Quasi-static and dynamic loading of fracture analysis on sandwich beams with a viscoelastic interface crack has been studied. Due to the viscoelastic nature of the interface on the fracture behavior of the sandwich material, it becomes important to also study the hysteresis effect. The fracture resistance can be improved by taking into consideration inertia effect where reasonable optimization of material parameters such as viscoelastic layer and the interfacial fracture toughness of composite sandwich can be improved (Anderson and Madenci, 2000b). The short-term mechanical behavior of both intact and preconditioned glass-fibre-reinforced composite sandwich I-beam under quasi-static loading has also been studied.

In terms of sandwich structure, sandwich panels made of graphite/epoxy face sheets with a polymethacrylimide foam core were subjected to a rigid spherical indenter in order to study the force-indentation response of the sandwich panels. To determine the contact pressure arising from static indentation by a rigid sphere as well as displacement fields in sandwich panel and the complete stress, a three-dimensional analytical solution method was developed. Major study in determining the core compressive stress that results from contact loading which is focusing on the accuracy of the contact analysis and the effect of sandwich parameters on the resulting core compressive stress due to the contact loading. An iterative solution scheme was utilized to determine the sphere's unknown contact area and pressure distribution due to indentation, unlike the usual assumption of a Hertzian-type contact pressure distribution. By performing quasi-static indentation experiments,

analytical predictions are validated and the accuracy of the prediction is established and the damage initiation in the face sheets and core were predicted from the present analysis which are in excellent agreement with the experimental results (Palazotto et al.,2000). The ability to model some of the important features of static indentation of composite sandwich structures was shown as a comparison to experimental low-velocity impact and static indentation data (Rios et al.,2007).

2.3.4 Tensile Test

Tensile test is carried out to determine the in-plane tensile properties of polymer matrix composite materials reinforced by high-modulus fibers. The composite material forms are limited to discontinuous fiber-reinforced composites or continuous fiber in which the laminate is symmetric and balanced with respect to the test direction. Standard test method used are ASTM D 3039, ASTM D 3878 and ASTM D 883, as for tensile properties of polymer matrix composite materials.

Equilibrium method of the tensile test is considered more advantageous over material law as it provides better transverse shear stresses. For the sandwich structure, the core will fail as a consequence of combined effect of shear and compression (Ahmed and Vijayarangan,2008). Aminanda et al (2009) have shown that microdebonding between the loop cross-over points in the woven fabric structure are the initial cause of damage. Initiation of the pattern and sites of cracking are closely related to the fabric orientation and architecture with respect to the loading direction which in turn develops matrix cracking damage (Castanié et al.,2008).